J Radioanal Nucl Chem (2010) 283:541–546
DOI 10.1007/s10967-009-0366-2

Adsorptivity of polyvinylpolypyrrolidone for selective separation of U(VI) from nitric acid media

M. Nogami · Y. Sugiyama · T. Kawasaki · M. Harada · Y. Morita · T. Kikuchi · Y. Ikeda

Received: 26 August 2009 / Published online: 11 September 2009

Abstract Adsorptivity of polyvinylpolypyrrolidone (PVPP), a candidate resin with selectivity to U(VI) in HNO_3 media, to various metal ions was examined. It was found that PVPP has a strong adsorptivity to U(VI) in wide concentration range of HNO_3. The Scatchard plot analysis revealed that the adsorption of U(VI) by PVPP occurs at plural binding sites. The infrared spectroscopic analysis suggested that the strong binding site is due to the coordination of the carbonyl oxygen atom and the nitrogen atom in the pyrrolidone ring to UO_2^{2+}. It was also found that fission product ions except Re(VII) as the simulant of Tc(VII) and Pd(II) are not adsorbed onto PVPP. The adsorptivities to Tc(VII) and Pd(II) species are weak, indicating that U(VI) can be separated from other metal ions by PVPP.

Keywords Polyvinylpolypyrrolidone · Monoamide · Resin · U(VI) · Pd(II) · HNO_3

Introduction

Uranium(VI) is the most stable U species in aqueous nitric acid solutions. Separation of U(VI) from HNO_3 containing U(VI) and other metal ions is very important to treat radioactive wastes. For developing resins with selectivity to U(VI) in HNO_3 media, we have synthesized several silica-supported polymer beads with the structure of a monoamide as the functional group and their adsorptivities to various metal ions have been examined [1–3].

Polyvinylpolypyrrolidone (PVPP) is one of the monoamide compounds and is a cross-linked form of water-soluble polyvinylpyrrolidone (PVP, Fig. 1). Thus, PVPP is insoluble in water. PVPP has been used in many fields such as plant tissue extraction [4], protein preparation [5], DNA extraction [6], and beverage clarification [7]. However, no studies have been made on the application of PVPP to the adsorbent of U(VI) in HNO_3 media.

We have already examined the adsorptivity of the silica-supported resins, Silica-VP, synthesized by polymerizing *N*-vinylpyrrolidone with a crosslinking agent and a porous silica support [2, 3]. Although the chemical structures of the functional groups of Silica-VP and PVPP are identical, the physical properties of the two kinds of resins are different. For example, swelling properties of the resins are different from each other due to presence and absence of the silica support. Therefore, studies on the adsorptivity of PVPP are expected to help the development of resins with selectivity to U(VI) in HNO_3 media. Based on the above background, the adsorptivities of PVPP to various metal ions were examined under various conditions.

Experimental

Commercial PVPP (SIGMA) was used as received without sieving. Adsorptivities of PVPP to U(VI) and major fission product (FP) ions in 0.1 to 6 mol/dm^3 (=M) HNO_3 solutions were examined by a batch method. The wet PVPP

M. Nogami (✉) · Y. Sugiyama · T. Kawasaki · M. Harada · Y. Ikeda
Research Laboratory for Nuclear Reactors, Tokyo Institute of Technology, 2-12-1-N1-34 O-okayama Meguro-ku, Tokyo 152-8550, Japan
e-mail: mnogami@nr.titech.ac.jp

Y. Morita
Japan Atomic Energy Agency, Tokai-mura, Naka-gun, Ibaraki 319-1195, Japan

T. Kikuchi
Mitsubishi Materials Corporation, Mukoyama, Naka-shi, Ibaraki 311-0102, Japan

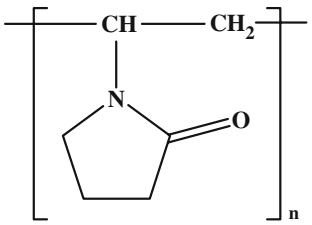

Fig. 1 Structure of PVPP

conditioned was contacted with the sample solution containing the metal ion and shaken vigorously at an appropriate interval at room temperature. Samples of the supernatant liquids were taken after the contact for maximum 100 h and the concentrations of the metal ions were measured by ICP-AES (Perkin Elmer, Optima 3000). The adsorptivity was evaluated by the distribution ratio, K_d, defined as,

$$K_d = \frac{C_o - C}{C} \times \frac{V}{W} \left(\mathrm{cm}^3/\mathrm{g}\right) \quad (1)$$

where C_0 and C denote the concentrations of the metal ion in the solution before and after contact with PVPP, respectively. V and W represent the volume of the solution and the weight of the dry PVPP, respectively.

Results and discussion

In order to examine the adsorption rate for U(VI), the amount of U(VI) adsorbed onto PVPP was measured at various time. The results are shown in Fig. 2, where q_U represents the amounts of adsorbed U(VI). This figure shows that the adsorption equilibrium is attained by ca. 20 min. The adsorptivities of PVPP to U(VI) and major FP ions are shown in Fig. 3. The U(VI) species are found to be

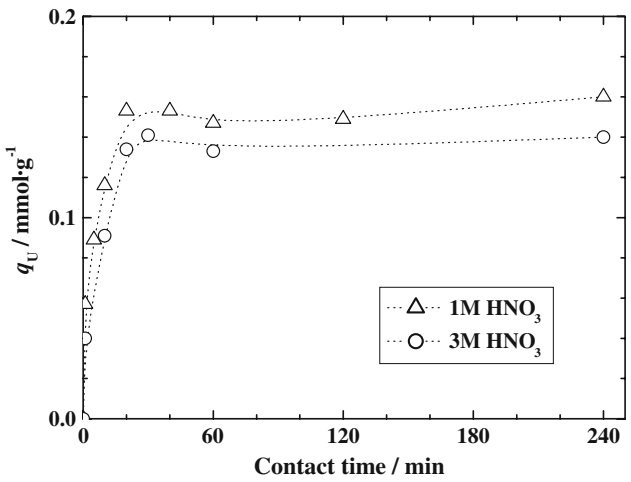

Fig. 2 Plots of amount of adsorbed U(VI) onto PVPP versus time. $[U(VI)]_{ini} = 5$ mM, 0.4 g PVPP/20 cm^3 sol

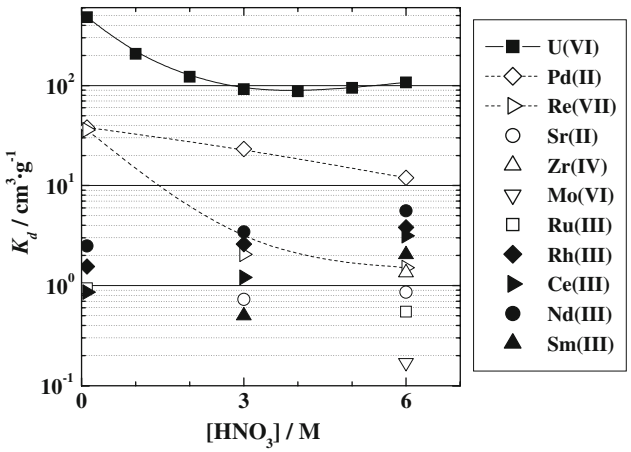

Fig. 3 Adsorptions of U(VI) and major FP ions onto PVPP from HNO_3 solutions. $[M]_{ini} = 0.831$–10 mM, 0.1–2 g PVPP/4–24 cm^3 sol, 30 h

strongly adsorbed onto PVPP in whole concentration range of HNO_3 in the present study. Particularly, the K_d values are larger in the lower concentration range (0.1–2 M) of HNO_3. Furthermore, it was found that Re(VII) as the simulant of Tc(VII) and Pd(II) are weakly adsorbed in the lower concentration range of HNO_3, where K_d values decreases with increasing concentrations of HNO_3. Other FP ions are found to be slightly adsorbed with K_d values smaller than 10. These results suggest that U(VI) can be separated from FP ions in HNO_3 media by normal column operations.

The adsorption isotherms for U(VI) in HNO_3 solutions from 0.1 to 5 M are shown in Fig. 4, where C_U* represents the equilibrium concentration of U(VI). The plots for lower concentration range of C_U* up to 25 mM of Fig. 4 was magnified (see Fig. 5). These figures indicate that the q_U values increase with decreasing concentrations of HNO_3 in the C_U* range less than ca. 8 mM. The inverse tendency is observed in the higher C_U* range. In the Silica-VP resins used in the previous study, the adsorptivity to U(VI) is little dependent on the concentrations of HNO_3 [2]. This is reasonably explained by the results in the present study, that is, the C_U* values in the experiments using Silica-VP were around 8 mM, where the adsorption isotherms of PVPP for various concentrations of HNO_3 overlap as seen from Fig. 5.

The above results indicate that PVPP can be effectively recycled for the treatment of solutions containing U(VI) of relatively high concentrations only by changing the concentrations of HNO_3, i.e., adsorption of U(VI) using HNO_3 solutions of high concentrations and elution of the adsorbed U(VI) using diluted HNO_3. It can be estimated from Fig. 4 that the adsorption capacity of PVPP for U(VI) is approximately 2.5 mmol/dry-g for 3 M HNO_3 system.

Scatchard plot analysis is widely used to investigate the characteristics of the adsorption process based on the

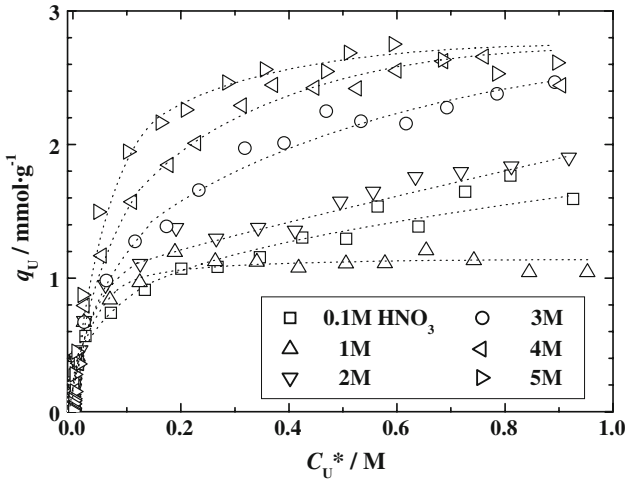

Fig. 4 Adsorption isotherms of PVPP for U(VI) in high concentration range of U(VI). $[U(VI)]_{ini}$ = 2–500 mM, 0.1 g PVPP/1–4 cm^3 sol, 3 h

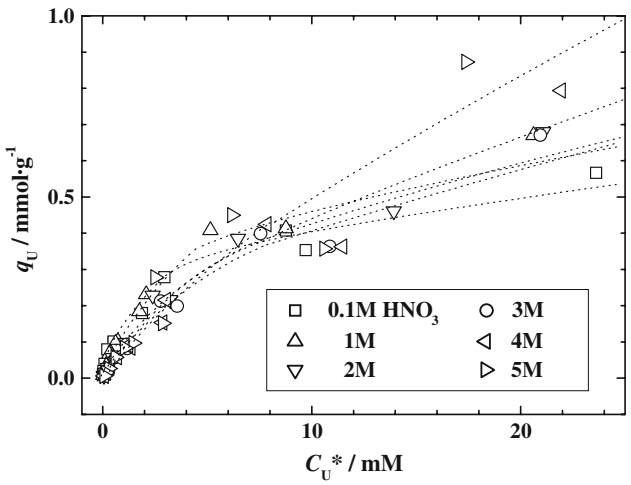

Fig. 5 Adsorption isotherms of PVPP for U(VI) in low concentration range of U(VI)

interactions between functional groups of resins and metal ions, and the shape of the plot is related to the types of interactions [8]. The Scatchard plots for the adsorption of U(VI) onto PVPP derived from Fig. 5 are shown in Fig. 6. All plots deviate from the linear negative line and show concave curves, indicating that the adsorption of U(VI) onto PVPP does not follow the linear Langmuir model. In addition, the slope in the region of small q_U values becomes steeper with decreasing concentrations of HNO_3. These facts suggest that the adsorption of U(VI) onto PVPP occurs at strong and weak binding sites, where the steeper slope represents the adsorption in the strong site [8]. It is also suggested that the contribution of the strong site increases with a decrease in the concentrations of HNO_3.

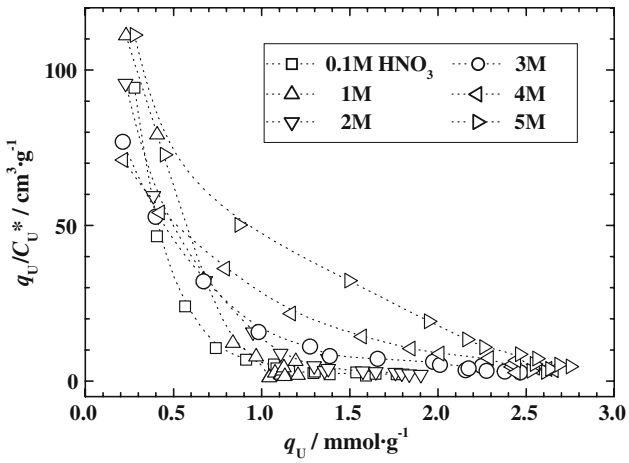

Fig. 6 Scatchard plots for binding of PVPP and U(VI)

Based on the result that PVPP has plural binding sites for U(VI), we applied the bi-Langmuir model to the present system. The bi-Langmuir isotherm equation is expressed as follows [9]:

$$q_U = q_{U(m1)}\frac{aC_U}{1+aC_U} + q_{U(m2)}\frac{bC_U}{1+bC_U} \quad (2)$$

where a and b are numerical parameters (M^{-1}), $q_{U(m1)}$ and $q_{U(m2)}$ represent the adsorption capacities at each adsorption site (mmol g^{-1}), respectively, and C_U is the concentration of U(VI) in the solution (M). The four parameters (a, b, $q_{U(m1)}$, $q_{U(m2)}$) can be estimated in the region where C_U* values are large enough, i.e., the total adsorption capacity $q_m = q_{U(m1)} + q_{U(m2)}$. Non-linear fitting of the theoretical isotherm of the bi-Langmuir model was performed in a wide concentration range of U(VI) (10^{-3}–0.2 M) for 0.1 and 3 M HNO_3, respectively. The results are listed in Table 1. The correlation coefficients (R) for both systems are found to be nearly one, supporting that the adsorptivity of U(VI) onto PVPP can be expressed by the bi-Langmuir model.

As discussed above, the contribution of the strong binding site decreases with increasing concentrations of HNO_3. However, as seen from Figs. 4 and 5, the maximum adsorption capacities of PVPP for U(VI) basically increase with an increase in the concentrations of HNO_3 in the C_U* range more than ca. 8 mM. Therefore, the predominant adsorption for U(VI) under higher concentrations of HNO_3 occurs due to a weak binding. More specifically, the binding may be the complex formation of UO_2^{2+} with two nitrate ions and two oxygen atoms of the carbonyl group of PVPP, i.e., $UO_2(NO_3)_2(C{=}O_{(PVPP)})_2$, according to our previous studies on the silica-supported resins [1, 2].

The adsoptivities of Re(VII) and Pd(II) are different from those of other fission product ions as shown in Fig. 3. It is reported that Tc(VII) is extracted from HNO_3 solutions

Table 1 Fitting parameters using bi-Langmuir model and correlation coefficients

HNO_3/M	*a*	*b*	$q_{U(m1)}$	$q_{U(m2)}$	*R*
0.1	1.82	359	5.94	0.483	0.9995
3	4.80	196	3.25	0.500	0.9999

of low concentrations by cyclic monoamide extractants and that the complex formation of $(HTcO_4)(amide)_{1–2}$ and $(HTcO_4)(amide)_{3–6}$ is proposed as the extraction mechanisms [10]. The chemical properties of Re(VII) are similar to those of Tc(VII). Thus, the Re(VII) species are considered to be adsorbed via the similar mechanism.

The adsorptivity of Pd(II) onto PVPP is unique. As shown in Fig. 7, the adsorption rates for Pd(II) are extremely slower than those for U(VI), where q_{Pd} represents the amount of adsorbed Pd(II). Such a slow adsorption of Pd(II) in HNO_3 media is also observed for an anion exchange resin consisting of tertiary *N*-methylbenzimidazole (ca. 40%) and quaternary *N,N′*-dimethylbenzimidazolium (ca. 60%) groups as the functional group. The slow adsorption found in 6 M HNO_3 at 333 K is explained by the slow complex formation between Pd(II) and the nitrogen atom of the anion exchange resin [11]. For PVPP, the color of the samples of 0.1 and 3 M HNO_3 was changed gradually from orange to dark brown with the adsorption of Pd(II). While, the sample of 6 M HNO_3 kept orange.

The time dependence of the Scatchard plots for the binding of PVPP and Pd(II) in 3 M HNO_3 is shown in Fig. 8, where C_{Pd} represents the concentration of Pd(II) in the solution. It can be seen that all plots deviate from the linear negative line and are clearly divided into two parts: a very steep linear line in the region of very small q_{Pd} values and a linear line with a gentle slope in the other region.

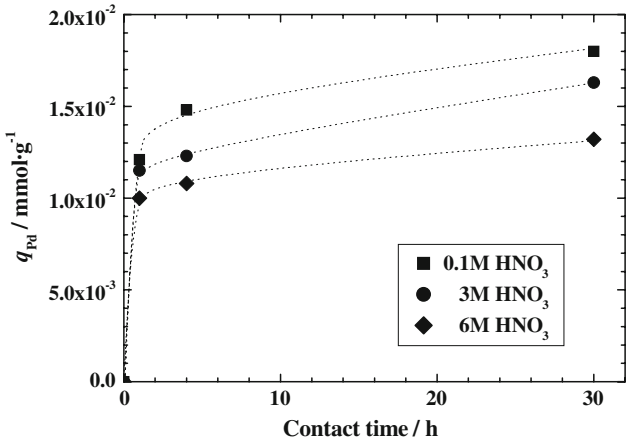

Fig. 7 Plots of amount of adsorbed Pd(II) onto PVPP versus time. $[Pd(II)]_{ini} = 1.89$ mM, 2 g PVPP/24 cm^3 sol

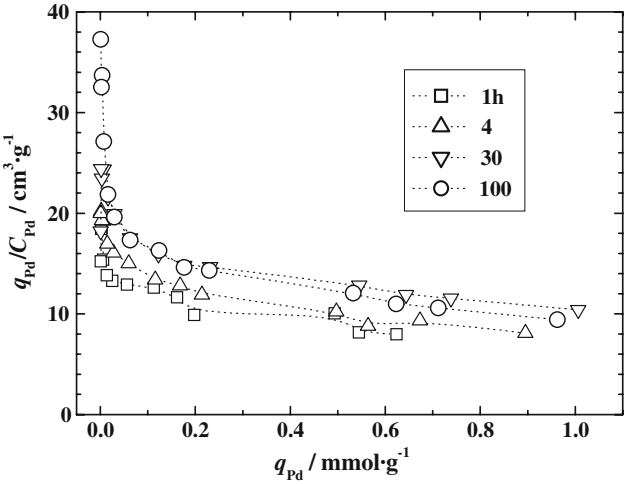

Fig. 8 Time dependence of Scatchard plots for binding of PVPP and Pd(II) in 3 M HNO_3

The contribution of the former part is found to remain very small in all adsorption sites of Pd(II) regardless of the time evolution.

Water-soluble PVP has been often used to obtain stable dispersions of metal nanoparticles, especially of Au, Ag, and platinum group [12–16]. It is known that the preparation of PVP-stabilized nanoparticles involves two processes: reduction of metal ions into neutral atoms, which form clusters, and coordination of the polymer to the metal clusters. Although there are a lot of synthetic methods to obtain the nanoparticles, the reduction of those metal ions by the simple mixing of PVP and the metal ion solution has been reported, where the following facts were found: (i) PVP has a strong reduction effect on free metal ions, such as Ag^+ ion in $AgNO_3$, and shows much weaker effect on metal complex ions, e.g., $AuCl_4^-$ in $HAuCl_4$ and $Ag(NH_3)_2OH$; (ii) the formation rate of Ag by the reduction of Ag^+ by PVP is three orders of magnitude higher than that of Au from Au^{3+}. Strong donor of the nitrogen and oxygen atoms in the polar group of PVP is proposed as the driving force of the reduction [16].

Considering the molar fraction of Pd(II)-nitrate species as a function of nitrate concentration [17], the predominant Pd(II) species in 0.1, 3, and 6 M HNO_3 are Pd^{2+} and $Pd(NO_3)^+$, $Pd(NO_3)^+$ and $[Pd(NO_3)_3]^-$, and $[Pd(NO_3)_3]^-$, respectively. These results indicate that the reduction of Pd(II) in our study proceeds more easily with decreasing concentrations of HNO_3. The color change in the appearance of the PVPP samples after adsorbing Pd(II) may be attributed to the reduction of Pd(II) to Pd(0) by the contact of Pd(II) with PVPP.

In fact, in our study, black fine powder was generated a few days after mixing 0.21 g of PVP (ACROS, K12, average M.W. 3500) and 4 cm^3 of Pd(II) standard solution

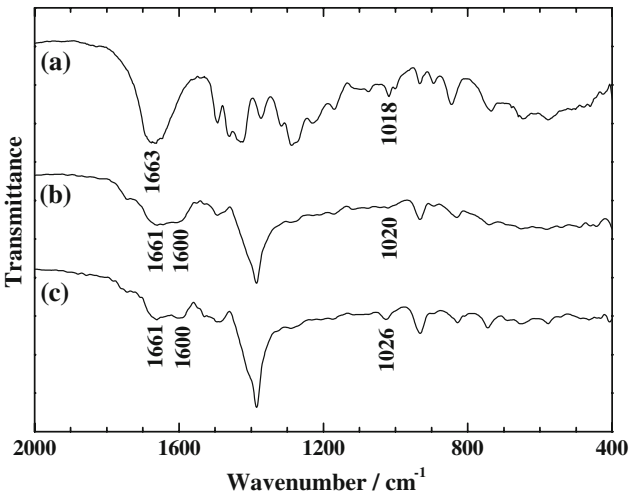

Fig. 9 Infrared spectra of neat PVPP and PVPP after adsorption of U(VI). **a** neat; **b** after adsorption of U(VI) from 0.1 M HNO_3; **c** after adsorption of U(VI) from 6 M HNO_3

(Kanto, 1000 ppm in 1 M HNO_3) at room temperature. However, the identification has not yet been successful due to very little amount of the powder. Alternatively, it is reported that the reduction of Ag^+ and Au^{3+} by PVP can be detected by the change in the UV–vis absorption spectra [12, 14–16]. In our corresponding experiment, apparent changes have not been observed in 0.1 M HNO_3 containing 10 mM PVP and 5 mM Pd(II).

From these results, it is suggested that the color changes in PVPP after adsorbing Pd(II) may occur in the minor adsorption site, although it has a strong binding property. On the other hand, it is suggested that the major adsorption site is related to the strong coordination field generated by the nitrogen and oxygen atoms in the polar group of PVPP, since no adsorption of Pd(II) was found for Silica-DMAA resins whose functional group is composed of straight chain acrylamide [1]. In addition, pyrrolidone derivatives such as *N*-cyclohexyl-2-pyrrolidone, *N*–*n*-octyl-2-pyrrolidone, and *N*–*n*-dodecyl-2-pyrrolidone are found to extract Pd(II) from HNO_3 solutions with a maximum K_d value at around 1–3 M [18]. The detailed adsorption form of the major site should be investigated in the future.

The similar discussion may be applied to the clarification of the strong binding site of U(VI) onto PVPP under lower concentrations of HNO_3. The infrared spectra of neat PVPP and that after adsorbing U(VI) are shown in Fig. 9. The PVPP samples adsorbing U(VI) were prepared by contacting 0.1 g of PVPP and 1 cm^3 of 0.1 or 6 M HNO_3 containing 100 mM U(VI), respectively. It can be seen that the peak at 1663 cm^{-1} before adsorption, which is attributed to the C=O bond in the pyrrolidone ring, is split into two peaks after adsorption (1661, 1600 cm^{-1}). This suggests that the adsorption of U(VI) onto PVPP occurs by the coordination of two oxygen atoms of the two amide groups to U(VI), forming $UO_2(NO_3)_2(C{=}O_{(PVPP)})_2$, as mentioned above.

In addition, the peak at 1018 cm^{-1} before adsorption, which is attributed to the C–N bond in the pyrrolidone ring, is significantly decreased in the sample after adsorption in 0.1 M HNO_3 (1020 cm^{-1}). On the other hand, the peak is still present at 1026 cm^{-1} in the sample adsorbing U(VI) from 6 M HNO_3. These results are similar to those obtained in PVP–$AgNO_3$ system [16], and indicate the contribution of the nitrogen atom in PVPP to the adsorption of U(VI) in HNO_3 solutions of low concentrations. This contribution is expected to decrease with increasing concentrations of HNO_3, because of the protonation of the nitrogen atom. Such an approach to clarify the nature of the C–N bond by IR spectrometry is impossible for the silica-supported resins, because a large absorption peak attributed to Si–O bond is observed in the range of approximately 900–1300 cm^{-1} in the silica support.

Conclusion

In the present study, the adsorptivity of PVPP to various metal ions was examined as a part of the development of resins selective to U(VI) in HNO_3 media. As a result, it was found that PVPP has a strong adsorptivity to U(VI) in HNO_3 solutions of wide concentration range with the plural adsorption sites. It was suggested that the strong binding site is the coordination of the carbonyl oxygen and nitrogen atoms in the pyrrolidone ring to UO_2^{2+}, and the weak one is the complex formation of UO_2^{2+} with two nitrate ions and two oxygen atoms of the carbonyl group of PVPP. The adsorption in the strong site appeared more clearly in lower concentration range of HNO_3 and is proposed to be due to the strong coordination of UO_2^{2+} with the nitrogen and oxygen atoms in the polar group of PVP.

Furthermore, it was found that the major FP ions except for Re(VII) and Pd(II) are not adsorbed onto PVPP. These two metal ions showed weak adsorptivity in HNO_3 solutions of lower concentrations. These results indicate that U(VI) can be separated from major FP ions by PVPP. The unique adsorptivity of Pd(II) was also explained by its strong coordination to PVP.

Acknowledgment Present study includes the result of "Development of Advanced Reprocessing Systen Based on Use of Pyrrolidone Derivatives as Novel Precipitants with High Selectivity and Controllability" entrusted to Tokyo Institute of Technology by the Ministry of Education, Culture, Sports, Science and Technology of Japan (MEXT).

References

1. Nogami M, Ishihara T, Suzuki K, Ikeda Y (2007) J Radioanal Nucl Chem 273:37–41
2. Nogami M, Ishihara T, Maruyama K, Ikeda Y (2008) Prog Nucl Energy 50:462–465
3. Nogami M, Sugiyama Y, Ikeda Y, J Radioanal Nucl Chem. doi: 10.1007/s10967-009-0137-0
4. Loomis WD (1974) Meth Enzymol 31-pt. A:528–544
5. Gaucher GM (1975) Meth Enzymol 43:540–548
6. Barns SM, Fundyga RE, Jeffries MW, Pace NR (1994) Proc Natl Acad Sci USA 91:1609–1613
7. Leiper KA, Stewart GG, McKeown IP, Nock T, Thompson MJ (2005) J Inst Brew 111:118–127
8. Ayar A, Mercimek B (2006) Proc Biochem 41:1553–1559
9. Holford ICR, Wedderburn RWM, Mattingly GEG (1974) Eur J Soil Sci 25:242–245
10. Suzuki S, Tamura K, Tachimori S, Usui Y (1999) J Radioanal Nucl Chem 239:377–380
11. Wei Y, Kumagai M, Takashima Y, Asou M, Namba T, Suzuki K, Maekawa A, Ohe S (1998) J Nucl Sci Technol 35:357–364
12. Zhang Z, Zhao B, Hu L (1996) J Solid State Chem 121:105–110
13. Zhang Y, Yang G, Li X, Luo W, Huang M, Jiang Y (1999) Poly Adv Technol 10:108–111
14. Carotenuto G, DeNicola S, Nicolais L (2001) J Nanopart Res 3:469–474
15. Pastoriza-Santos I, Liz-Marzán LM (2002) Langmuir 18:2888–2894
16. Kan C, Cai W, Li C, Zhang L (2005) J Mater Res 20:320–324
17. El-Reefy SA, Daoud JA, Aly HF (1992) J Radioanal Nucl Chem 158:303–312
18. Takahashi Y, Hotokezaka H, Noda K, Ikeda Y (Aug 2008) 7th International Conference Nuclear and Radiochemistry (NRC7), Budapest, Hungary, PB47